Excitation of the hyperfine levels of 13CN and C15N in collisions with H2 at low temperatures

D. Flower, F. Lique

Monthly Notices
of the
ROYAL ASTRONOMICAL SOCIETY

MNRAS **446,** 1750–1755 (2015) doi:10.1093/mnras/stu2231

Excitation of the hyperfine levels of ^{13}CN and C^{15}N in collisions with H_2 at low temperatures

D. R. Flower[1]★ and F. Lique[2]

[1]*Physics Department, The University, Durham DH1 3LE, UK*
[2]*LOMC–UMR 6294, CNRS–Université du Havre, 25 rue Philippe Lebon. BP 1123, F-76 063 Le Havre cedex, France*

Accepted 2014 October 22. Received 2014 October 21; in original form 2014 October 8

ABSTRACT

Cross-sections and rate coefficients for transitions between the fine and hyperfine levels of the isotopologues, ^{13}CN, and C^{15}N, of the CN radical, induced by collisions with para-H_2 in its rotational ground state, $j = 0$, have been computed. The effects of the isotopic shift of the centre of mass on the interaction potential were included, and energy levels specific to each isotopologue were used. The isotopologue-dependence of the results was found to be such that we recommend that rate coefficients specific to each isotopologue should be used when analysing observations of hyperfine transitions. The numerical values of the rate coefficients are available for kinetic temperatures $T \lesssim 10^2$ K.

Key words: molecular data – molecular processes – scattering.

1 INTRODUCTION

CN is one of the trio of interstellar molecular species – CN, CH, and CH^+ – that were observable in the visible part of the spectrum, through electronic transitions, prior to the advent of radio telescopes. Subsequently, its rotational transitions have been observed extensively, and modern spectrometers are able to resolve the hyperfine structure of the rotational transitions of CN, which arises from the non-zero spin of the N-nucleus. Observations of CN have assumed particular importance in the context of low-mass star formation, as CN is present in the pre-stellar cores as a gas-phase species, even at the low temperatures (of the order of 10 K) which prevail in these sources (cf. Hily-Blant et al. 2008). In order to interpret such observations, the rates of excitation of the hyperfine levels of CN by its principal collision partner, para-H_2, are required and were calculated by Kalugina, Lique & Klos (2012). More recently, rate coefficients for the excitation of CN by ortho-H_2 have also been computed (Kalugina & Lique 2015).

The interpretation of the observations of CN is complicated by the fact that its transitions can become optically thick. This problem may be avoided by using, instead, the lines of ^{13}CN and C^{15}N, which are also observable. However, these isotopic species have total nuclear spins of $I = \frac{1}{2}$ or $I = \frac{3}{2}$, in the case of ^{13}CN, and $I = \frac{1}{2}$, in the case of C^{15}N, which differ from the spin ($I = 1$) of the most abundant isotopologue. It follows that the cross-sections for transitions between the hyperfine levels of ^{13}CN and C^{15}N have to be computed separately from those for CN. Furthermore, the isotopic shifts of the centre of mass have consequences for the potential of interaction of CN with the H_2 molecule, and hence for the cross-sections for transitions between the fine-structure states of CN, induced by collisions with H_2. These issues are addressed in this paper.

In Section 2, we present the results of calculations of cross-sections and rate coefficients for transitions between hyperfine states of ^{13}CN and C^{15}N, induced by collisions with para-H_2 in its rotational ground state. The quantum–mechanical coupled-channels (CC) method was used to calculate the scattering matrix for transitions between the fine-structure states of ^{13}CN and C^{15}N, from which the hyperfine cross-sections were derived by means of the appropriate algebraic transformation. Our concluding remarks are made in Section 3.

2 CALCULATIONS

2.1 Interaction potential

We adopted the same CN–H_2 ab initio interaction potential as Kalugina et al. (2012). The H_2 molecule is taken to be in the $j = 0$ rotational ground state of its para modification, in which case it can be treated as a pseudo-closed-shell atom, analogous to He. In order to use this potential consistently for ^{13}CN–H_2 and C^{15}N–H_2 collisions, it is necessary to allow for the shift of the centre of mass of the radical, arising from the isotopic substitutions, when expanding the potential, $V(R, \theta)$, in terms of Legendre polynomials, $P_\lambda(\theta)$,

$$V(R, \theta) = \sum_\lambda v_\lambda(R) P_\lambda(\theta), \quad (1)$$

where R is the separation of the centre of mass of the radical and the pseudo-atom and θ is the angle between the intermolecular and intramolecular vectors.

★ E-mail: david.flower@durham.ac.uk

The shifts of the centre of mass in the cases of ^{13}CN and C^{15}N are 2.0 and 1.7 per cent of the bond length, towards the ^{13}C and the ^{15}N atoms, respectively, Although these shifts are modest, it should be recalled that they are in opposite directions.

The reduced mass of the molecule also changes. We allow for the effect of this change on the energies of the fine-structure levels by using isotopologue-specific values: see Section 2.2. The change in the reduced nuclear mass modifies also the vibrational energies and wave functions, and hence the vibrationally averaged value of the internuclear separation. However, this effect – which we expect to be small compared with that of the centre-of-mass shift – is not taken into account in the present calculations, which assume the same internuclear separation for ^{13}CN and C^{15}N as for CN.

The potentials for ^{13}CN–H$_2$ and C^{15}N–H$_2$ were obtained on the same grid of values of R and θ as the CN–H$_2$ potential by generating the latter at the appropriately shifted grid points, determined by simple trigonometry. Terms with $0 \leq \lambda \leq 8$ on a grid of intermolecular distances $R = 4.50(0.25)16.00\ a_0$ were used. Beyond 16 a_0, all the $v_\lambda(R)$ except $v_0(R)$, $v_1(R)$, and $v_2(R)$ were damped exponentially to zero, with the three leading terms being matched to R^{-6}, R^{-7}, and R^{-6}, respectively, long-range forms at $R = 16\ a_0$.

The potential expansion coefficients, $v_\lambda(R)$, with $0 \leq \lambda \leq 3$, are plotted in Fig. 1 for the three cases of CN–para-H$_2$, ^{13}CN–para-H$_2$, and C^{15}N–para-H$_2$, where the para-H$_2$ molecule is taken to be in its rotational ground state; the uppermost panel corresponds to fig. 3 of Kalugina et al. (2013). It may be seen from Fig. 1 that the anisotropic terms, v_1, v_2, v_3 – which intervene directly in inelastic scattering – are modified by the centre-of-mass shifts, whereas the isotropic term, v_0, is not noticeably affected.

As may be seen in Fig. 1, the isotopic shifts in the centre of mass affect disproportionately the expansion coefficients for which λ is odd (plotted as the broken curves). These coefficients are responsible directly for transitions, induced by para-H$_2$($j = 0$), in which the change in the rotational quantum number, ΔN, is odd. We shall see in Section 2.3 that the cross-sections for such transitions have the greatest sensitivity to the identity of the isotopologue.

2.2 Inelastic collisions

2.3 Neglecting the nuclear spin

We have studied the rotationally inelastic scattering of CN (and its isotopologues) on para-H$_2$($j = 0$) by means of both the HIBRIDON[1] and MOLCOL (Flower, Bourhis & Launay 2000) CC scattering codes, which yielded identical cross-sections, to within the numerical precision of the calculations. With the exception of the $N = 0$ ground state, each rotational state of CN is split into an energetically close doublet of fine-structure states, $j = N - \frac{1}{2}$ and $j = N + \frac{1}{2}$, by the interaction between the rotational angular momentum, $\boldsymbol{N}$, and the net electron spin angular momentum, $\boldsymbol{S}$, where $S = \frac{1}{2}$. We included states $0 \leq N \leq 12$ in our rotational basis. The energies were calculated using the spectroscopic constants determined Bogey, Demuynck & Destombes (1984) and Saleck, Simon & Winnewisser (1994) for ^{13}CN and C^{15}N, respectively; the energies are listed in Table 1.

In Table 2, representative cross-sections – for transitions into the $(N, j) = (0, \frac{1}{2})$ ground fine-structure state from higher states – are given for two collision energies, $E = 60$ and 100 cm^{-1}, at which

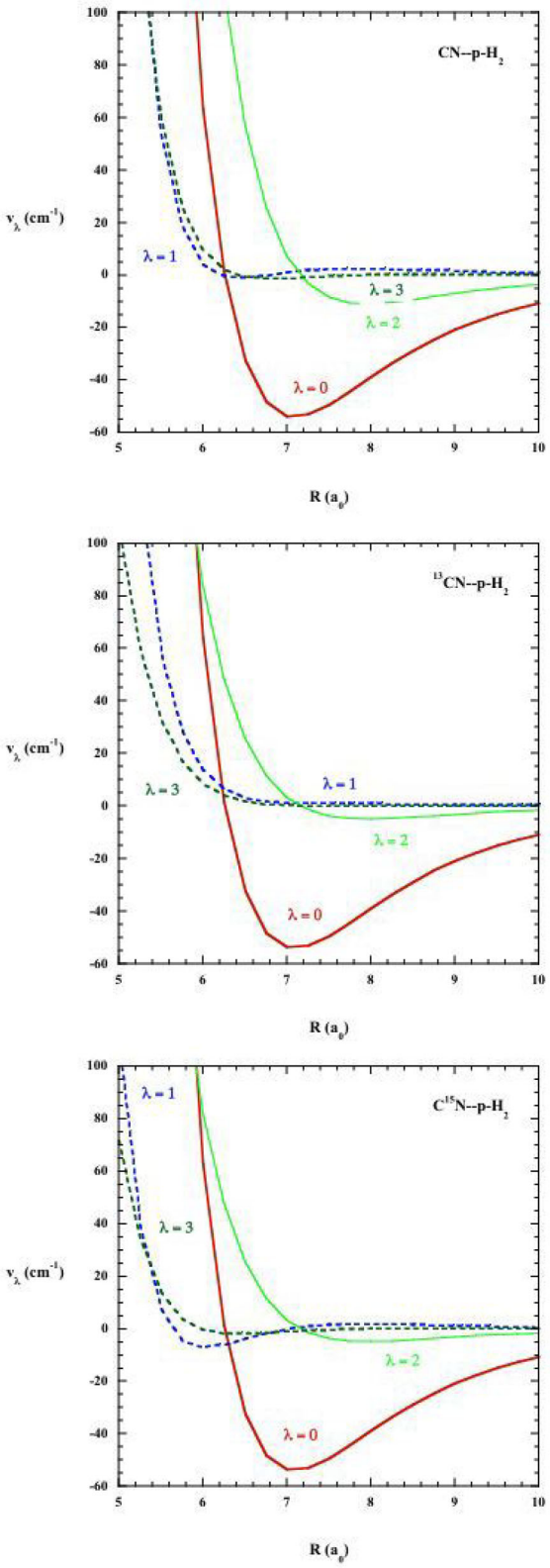

Figure 1. The four lowest order expansion coefficients, $v_\lambda(R)$, of the CN–p-H$_2$, ^{13}CN–p-H$_2$, and C^{15}N–p-H$_2$ interaction potentials, as functions of the intermolecular distance, $5 \leq R \leq 10\ a_0$.

[1] http://www2.chem.umd.edu/groups/alexander/hibridon/hib43/

Table 1. Energies (in cm^{-1}; $1\,cm^{-1} \equiv 1.4388$ K) of the states (N, j), $0 \le N \le 12$. of ^{13}CN and $C^{15}N$, calculated using the spectroscopic constants of Bogey et al. (1984) and Saleck et al. (1994), respectively.

(N, j)	^{13}CN	$C^{15}N$
$(0, \frac{1}{2})$	0.000	0.000
$(1, \frac{1}{2})$	3.618	3.659
$(1, \frac{3}{2})$	3.629	3.670
$(2, \frac{3}{2})$	10.866	10.989
$(2, \frac{5}{2})$	10.883	11.006
$(3, \frac{5}{2})$	21.739	21.984
$(3, \frac{7}{2})$	21.764	22.008
$(4, \frac{7}{2})$	36.239	36.644
$(4, \frac{9}{2})$	36.270	36.676
$(5, \frac{9}{2})$	54.365	54.970
$(5, \frac{11}{2})$	54.403	55.009
$(6, \frac{11}{2})$	76.119	76.960
$(6, \frac{13}{2})$	76.164	77.006
$(7, \frac{13}{2})$	101.501	102.613
$(7, \frac{15}{2})$	101.554	102.666
$(8, \frac{15}{2})$	130.513	131.928
$(8, \frac{17}{2})$	130.572	131.988
$(9, \frac{17}{2})$	163.155	164.905
$(9, \frac{19}{2})$	163.221	164.972
$(10, \frac{19}{2})$	199.429	201.541
$(10, \frac{21}{2})$	199.502	201.615
$(11, \frac{21}{2})$	239.336	241.836
$(11, \frac{23}{2})$	239.416	241.917
$(12, \frac{23}{2})$	282.878	285.788
$(12, \frac{25}{2})$	282.965	285.876

levels with $N \le 5$ and $N \le 6$, respectively, are energetically accessible. Results are shown for collisions with CN, ^{13}CN, and $C^{15}N$; the CC approximation was used in these and subsequent calculations. It may be seen from this table that there are non-negligible differences between the cross-sections for the same transition in different isotopologues, particularly when ΔN is odd. On the other hand, cross-sections for transitions in which ΔN is even tend to be larger.

2.4 Including the nuclear spin

The angular momentum $\boldsymbol{j} = \boldsymbol{N} + \boldsymbol{S}$ is only weakly coupled to the net nuclear spin angular momentum, $\boldsymbol{I}$, and this interaction gives rise to correspondingly small splittings of the fine-structure energy levels,[2] identified by (N, j), into levels that are distinguished by the values of the total angular momentum of the molecule, $\boldsymbol{F} = \boldsymbol{j} + \boldsymbol{I}$. Denoting the relative angular momentum of the CN and para-H_2 molecules by $\boldsymbol{\ell}$, the total angular momentum of the colliding system, neglecting the nuclear spin, is $\boldsymbol{J} = \boldsymbol{j} + \boldsymbol{\ell}$, and the total angular momentum, including the nuclear spin, is $\boldsymbol{J}_{\rm tot} = \boldsymbol{J} + \boldsymbol{I}$.

[2] The hyperfine splittings are typically two orders of magnitude smaller than the fine splittings.

The transition matrix, $\mathbf{T}$, from which the collision cross-sections are directly derived, is calculated neglecting nuclear spin, and then the nuclear spin is incorporated by means of a unitary transformation to $\mathbf{T}'$, of the form

$$\mathbf{T}' = \mathbf{A}\mathbf{T}\mathbf{A}^{-1}, \tag{2}$$

where the (real) elements of the unitary matrix $\mathbf{A}$ are given by

$$A(I, j, F, 0, \ell, \ell, I, J, J_{\rm tot}) = [(2F+1)(2\ell+1)(2I+1)(2J+1)]^{1/2} \begin{Bmatrix} I & j & F \\ 0 & \ell & \ell \\ I & J & J_{\rm tot} \end{Bmatrix} \tag{3}$$

and where the array in curly brackets is a $9j$ angular momentum coupling coefficient (see, for example, Edmonds 1974); we note that the zero element of the $9j$ coefficient is the value of the net nuclear spin of the para-H_2 molecule. Thus, the cross-sections for transitions between hyperfine states may be determined by means of a purely algebraic transformation of the matrix for transitions between fine-structure states, (N, j). In the case of ^{13}CN, the transformations may be performed independently for each of the two possible values of the total nuclear spin, $I = \frac{1}{2}$ and $I = \frac{3}{2}$.

For CN colliding with para-H_2, we have compared hyperfine cross-sections derived by means of the above transformation with results obtained independently, following the approach of Daniel, Dubernet & Meuwly (2004), and found excellent agreement. A further (necessary but not sufficient) condition is that the summation rules

$$\sum_F \Omega(N'j'F', NjF) = \frac{(2F'+1)}{(2j'+1)} \Omega(N'j', Nj) \tag{4}$$

and hence

$$\sum_{F',F} \Omega(N'j'F', NjF) = (2I+1)\Omega(N'j', Nj) \tag{5}$$

should be satisfied; Ω is a dimensionless quantity, symmetric in the initial and the final states of the transition and related to the corresponding cross-section, σ, by

$$\pi\,\Omega(i, j) = k_i^2 \omega_i \sigma(i \to j). \tag{6}$$

In equation (6), $k_i^2 = 2\mu E_i/\hbar^2$ is the square of the wavenumber in the initial channel, i, and μ is the reduced mass of the CN–H_2 system; the degeneracies of the levels (N, j) are $\omega = (2j+1)$ and of the hyperfine levels (N, j, F) are $\omega = (2F+1)$.

2.5 Rate coefficients

The rate coefficient for the transition $i \to j$ is related to the corresponding cross-section by

$$q(i \to j) = \left(\frac{8k_{\rm B}T}{\pi\mu}\right)^{1/2} \int_0^\infty x_i \sigma(x_i | i \to j) {\rm e}^{-x_i} {\rm d}x_i, \tag{7}$$

where $x_i = E_i/k_{\rm B}T$ and T is the kinetic temperature. Rate coefficients for inverse transitions satisfy the detailed balance relation:

$$\omega_j q(j \to i) = \omega_i q(i \to j) \exp\left(\frac{E_j - E_i}{k_{\rm B}T}\right). \tag{8}$$

Introducing the dimensionless quantity, Ω, and substituting the numerical values of the constants yield

$$\omega_j q(j \to i) = \frac{1.11 \times 10^{-10}}{T^{\frac{1}{2}}} \int_0^\infty \Omega(x_j | j, i) {\rm e}^{-x_j} {\rm d}x_j, \tag{9}$$

Table 2. Cross-sections, in units of 10^{-16} cm^2, for transitions into the $(N, j) = (0, \frac{1}{2})$ ground state from each of the states (N, j) listed. From top to bottom: three sets of cross-sections are given for para-$H_2(j = 0)$ colliding with CN, ^{13}CN, and $C^{15}N$, respectively, at two collision energies, $E = 60$ and 100 cm^{-1}.

$(1, \frac{1}{2})$	$(1, \frac{3}{2})$	$(2, \frac{3}{2})$	$(2, \frac{5}{2})$	$(3, \frac{5}{2})$	$(3, \frac{7}{2})$	$(4, \frac{7}{2})$	$(4, \frac{9}{2})$	$(5, \frac{9}{2})$	$(5, \frac{11}{2})$	$(6, \frac{11}{2})$	$(6, \frac{13}{2})$
					60 cm^{-1}						
3.538(−1)	3.537(−1)	2.815	2.818	3.028(−2)	3.095(−2)	2.004(−1)	1.999(−1)	2.668(−2)	2.716(−2)		
3.454(−1)	3.453(−1)	2.817	2.819	2.681(−2)	2.708(−2)	1.990(−1)	1.985(−1)	3.844(−2)	3.920(−2)		
4.404(−1)	4.403(−1)	2.811	2.813	4.179(−2)	4.213(−2)	2.026(−1)	2.023(−1)	1.811(−2)	1.831(−2)		
					100 cm^{-1}						
2.165(−1)	2.165(−1)	2.822	2.823	5.792(−3)	5.798(−3)	1.642(−1)	1.643(−1)	6.655(−3)	6.652(−3)	1.885(−2)	1.892(−2)
2.380(−1)	2.381(−1)	2.805	2.806	1.425(−2)	1.425(−2)	1.623(−1)	1.624(−1)	9.553(−3)	9.553(−3)	1.858(−2)	1.864(−2)
2.768(−1)	2.769(−1)	2.831	2.832	9.452(−3)	9.464(−3)	1.661(−1)	1.662(−1)	5.121(−3)	5.116(−3)	1.900(−2)	1.906(−2)

Table 3. Cross-sections, in units of 10^{-16} cm^2, for transitions out of the $(N, j, F) = (0, \frac{1}{2}, 0)$ ground state into each of the states (N, j, F) listed. From top to bottom: two sets of cross-sections are given for para-$H_2(j = 0)$ colliding with ^{13}CN $(I = \frac{1}{2})$, and $C^{15}N$, respectively, at three collision energies, $E = 10$, 20, and 100 cm^{-1}. Numbers in parentheses are powers of 10.

$(0, \frac{1}{2}, 1)$	$(1, \frac{1}{2}, 0)$	$(1, \frac{1}{2}, 1)$	$(1, \frac{3}{2}, 1)$	$(1, \frac{3}{2}, 2)$	$(2, \frac{3}{2}, 1)$	$(2, \frac{3}{2}, 2)$	$(2, \frac{5}{2}, 2)$	$(2, \frac{5}{2}, 3)$
				10 cm^{-1}				
7.372(−1)	0.000	2.089	5.570	1.253(−2)				
4.688(−3)	0.000	8.425(−1)	1.675	4.609(−5)				
				20 cm^{-1}				
6.866(−3)	0.000	2.002	4.048	7.922(−4)	2.559(−4)	6.637	9.563	1.846(−3)
2.573(−3)	0.000	1.115	2.247	1.825(−4)	9.556(−5)	4.368	6.328	4.676(−4)
				100 cm^{-1}				
1.127(−8)	0.000	2.293(−1)	4.586(−1)	1.589(−9)	3.846(−9)	4.968	7.452	6.344(−9)
1.043(−4)	0.000	2.688(−1)	5.376(−1)	2.525(−9)	4.993(−9)	4.997	7.496	4.909(−9)

where T is in K and q in cm^3 s^{-1}. The rate coefficients were determined by numerical quadrature on a fine grid of collision energies.

Owing to the nuclear spin degeneracy of $(2I + 1)$, $\frac{1}{3}$ of the ^{13}CN molecules are in the $I = \frac{1}{2}$ state and $\frac{2}{3}$ are in the $I = \frac{3}{2}$ state; these weightings must be incorporated when calculating the total rate per unit volume of transitions between pairs of hyperfine states, F, F', $n(H_2 j = 0)n(^{13}CN)q(F \rightarrow F')$, where n denotes a number density and

$$q(F \rightarrow F') = \frac{1}{3} q\left(I = \frac{1}{2} \middle| F \rightarrow F'\right) + \frac{2}{3} q\left(I = \frac{3}{2} \middle| F \rightarrow F'\right). \quad (10)$$

When the rate coefficient is given in units of cm^3 s^{-1}, the number density is in cm^{-3}.

In Table 3, we compare cross-sections for the extreme cases of para-$H_2(j = 0)$ colliding with ^{13}CN $(I = \frac{1}{2})$, and $C^{15}N$, at three collision energies, $E = 10$, 20, and 100 cm^{-1}. We recall that there are differences in the interaction potentials in these two cases, arising from the centre-of-mass shifts, and differences in the spectroscopic constants and hence in the energy levels. At the highest collision energy, the numerical values of (particularly the largest) cross-sections are similar, with the exception of the quasi-elastic transition $(0, \frac{1}{2}, 0) \rightarrow (0, \frac{1}{2}, 1)$. At the lower collision energies, there are discrepancies, which can be large; these relate to differences in the resonance structures in the cross-sections.

Rate coefficients between hyperfine states have been calculated for ^{13}CN, $I = \frac{1}{2}$ and $I = \frac{3}{2}$, for kinetic temperatures $5 \leq T \leq 75$ and for $C^{15}N$ over the more extended temperature range $5 \leq T \leq 150$; in both cases the colliding partner is para-H_2 in its $j = 0$ rotational ground state. These results will be made available on the LAMDA[3] (Schöier et al. 2005) and BASECOL[4] (Dubernet et al. 2013) websites.

By way of illustration of these results, we compare, in Table 4, the rate coefficients calculated for para-$H_2(j = 0)$ colliding with ^{13}CN $(I = \frac{1}{2})$, and $C^{15}N$; transitions out of the $(N, j, F) = (1, \frac{3}{2}, 1)$ excited hyperfine state into a sequence of states (N, j, F) are listed. As might have been anticipated in the light of the discussion above, the values of the rate coefficients for the two isotopic variants of CN are similar but not identical.

3 CONCLUDING REMARKS

We have calculated cross-sections and rate coefficients for fine and hyperfine transitions of the isotopologues, ^{13}CN, and $C^{15}N$, of the CN radical, induced by collisions with para-$H_2(j = 0)$. We allowed for the effects of the centre-of-mass shift on the interaction potential and used isotopologue-specific energies of the levels. We found that the isotopologue-specific results differed from each other to an extent that may be significant to the analysis of observations of the (optically thin) hyperfine transitions of these species. The numerical values of the rate coefficients are being made available through the LAMDA and BASECOL websites or may be requested directly from the authors.

When the H_2 molecule is constrained to its $j = 0$ rotational state, as here, it assimilates to a closed-shell atom. Then, the dimensionality of the problem is reduced, as the calculations are independent

[3] http://home.strw.leidenuniv.nl/
[4] http://basecol.obspm.fr/

Table 4. Rate coefficients, in units of cm^3 s^{-1}, for transitions out of the $(N, j, F) = (1, \frac{3}{2}, 1)$ excited state into each of the states (N, j, F) listed. From top to bottom: two sets of rate coefficients are given for para-$H_2(j = 0)$ colliding with ^{13}CN ($I = \frac{1}{2}$), and C^{15}N, respectively, at three temperatures, $T = 10$, 20, and 50 K. Numbers in parentheses are powers of 10.

$(0, \frac{1}{2}, 0)$	$(0, \frac{1}{2}, 1)$	$(1, \frac{1}{2}, 0)$	$(1, \frac{1}{2}, 1)$	$(1, \frac{3}{2}, 1)$	$(1, \frac{3}{2}, 2)$	$(2, \frac{3}{2}, 1)$	$(2, \frac{3}{2}, 2)$	$(2, \frac{5}{2}, 2)$	$(2, \frac{5}{2}, 3)$
				10 K					
3.24(−12)	1.64(−12)	1.76(−12)	1.26(−11)	1.02(−9)	8.09(−12)	5.42(−13)	7.24(−13)	4.45(−12)	3.84(−13)
3.21(−12)	1.62(−12)	2.38(−12)	1.29(−11)	1.04(−9)	9.82(−12)	6.24(−13)	7.29(−13)	5.18(−12)	4.05(−13)
				20 K					
3.59(−12)	1.82(−12)	1.55(−12)	1.69(−11)	1.09(−9)	1.00(−11)	8.87(−13)	1.10(−12)	7.41(−12)	5.82(−13)
3.31(−12)	1.67(−12)	1.95(−12)	1.58(−11)	1.10(−9)	1.04(−11)	1.19(−12)	1.22(−12)	1.01(−11)	6.79(−13)
				50 K					
3.40(−12)	1.73(−12)	1.07(−12)	2.20(−11)	1.68(−9)	1.21(−11)	9.09(−13)	1.10(−12)	7.82(−12)	5.51(−13)
2.89(−12)	1.45(−12)	9.46(−13)	2.08(−11)	1.67(−9)	1.15(−11)	1.14(−12)	9.59(−13)	1.03(−11)	5.04(−13)

of the orientation of the H_2 internuclear axis. In the case of H_2–CN collisions, a full-dimensional study has been undertaken recently by Kalugina & Lique (2015). These authors found that the differences between the results of the reduced- and full-dimensional calculations of rate coefficients for transitions between hyperfine levels were typically less than 20–30 per cent over the range of temperature considered here. Furthermore, the differences decrease as the magnitudes of the rate coefficients increase. Thus, we are confident of the reliability of the rate coefficients that we have computed, particularly for the dominant transitions.

Hily-Blant et al. (2013) have calculated rate coefficients for the excitation of hyperfine levels of ^{13}CN and C^{15}N by para-H_2, using the infinite-order-sudden (IOS) approximation, which is expected to become more reliable as the collision energy increases (equivalently, as the temperature of the gas increases); for the case of CN–para-H_2, the calculations of Faure & Lique (2012) had confirmed this behaviour. However, at $T = 10$ K, which is characteristic of both cold molecular clouds and pre-stellar cores, the IOS and CC results were found to agree to within only a factor of about 3, which adds considerably to the uncertainties in the analysis of observations. In Appendix A, we compare the values of rate coefficients, calculated at $T = 10$, 30, and 80 K, computed using the CC (present results) and the IOS (Hily-Blant et al. 2013) methods.

Daniel et al. (2013) have computed rate coefficients for the excitation of ^{13}CN and C^{15}N by He. However, reduced-mass scaling of these results to the case of excitation by para-H_2 has been shown to be unreliable, particularly at low temperatures (Kalugina & Lique 2015). We conclude that the present results should be used when analysing observations of the isotopologues of CN in, notably, pre-stellar cores.

ACKNOWLEDGEMENTS

DRF acknowledges support from STFC (ST/L00075X/1), including provision of local computing resources. FL thanks the CPER Haute-Normandie/CNRT/Energie, Electronique, Matériaux, and the CNRS national programme 'Physique et Chimie du Milieu Interstellaire'. We thank Alexandre Faure for providing the IOS results in the appendix.

REFERENCES

Bogey M., Demuynck C., Destombes J. L., 1984, J. Chem. Phys., 121, 4540
Daniel F., Dubernet M.-L., Meuwly M., 2004, A&A, 480, L5
Daniel F. et al., 2013, A&A, 560, A3
Dubernet M.-L. et al., 2013, A&A, 553, A50
Edmonds A. R., 1974, Angular Momentum in Quantum Mechanics, Princeton University Press, Princeton, NJ
Faure A., Lique F., 2012, MNRAS, 425, 740
Flower D. R., Bourhis G., Launay J.-M., 2000, Comput. Phys. Commun., 131, 187
Hily-Blant P., Walmsley C. M., Pineau des Forêts G., Flower D. R., 2008, A&A, 480, L5
Hily-Blant P., Pineau des Forêts G., Faure A., Le Gal R., Padovani M., 2013, A&A, 557, A65
Kalugina Y., Klos J., Lique F., 2013, J. Chem. Phys., 139, 074301
Kalugina Y., Lique F., 2015, MNRAS, 446, L21
Kalugina Y., Lique F., Klos J., 2012, MNRAS, 422, 812
Saleck A. H., Simon R., Winnewisser G., 1994, ApJ, 436, 176
Schöier F. L., Van der Tak F. F. S., Van Dishoeck E. F., Black J. H., 2005, A&A, 432, 369

APPENDIX A: A COMPARISON OF CC AND IOS VALUES OF RATE COEFFICIENTS FOR ^{13}CN–PARA-H_2 AND C^{15}N–PARA-H_2

In Tables A1 and A2, we compare the present (CC) values of rate coefficients with those of Hily-Blant et al. (2013), who used the IOS approximation. For ^{13}CN–para-H_2, there is a difference in the adopted angular momentum coupling schemes.[5] Where both $I = \frac{1}{2}$ and $I = \frac{3}{2}$ contribute to a given transition in Table A1, which is the case of the fourth and fifth entries, we weight their contributions by $\frac{1}{3}$ and $\frac{2}{3}$, respectively (cf. equation 10).

It may be seen from this comparison that, whilst the overall agreement of the CC and IOS values is satisfactory, substantial discrepancies occur for some transitions.

[5] We used $\boldsymbol{j} = \boldsymbol{N} + \boldsymbol{S}$, $\boldsymbol{I} = \boldsymbol{I}_1 + \boldsymbol{I}_2$. $\boldsymbol{F} = \boldsymbol{j} + \boldsymbol{I}$, whereas Hily-Blant et al. used $\boldsymbol{j} = \boldsymbol{N} + \boldsymbol{S}$, $\boldsymbol{F}_1 = \boldsymbol{j} + \boldsymbol{I}_1$, $\boldsymbol{F} = \boldsymbol{F}_1 + \boldsymbol{I}_2$, where $I_1 = \frac{1}{2}$ is the spin of the ^{13}C nucleus and $I_2 = 1$ is the spin of the N nucleus.

Table A1. Illustrative comparisons of rate coefficients ($cm^3\ mol^{-1}\ s^{-1}$) for hyperfine transitions in ^{13}CN, induced by para-$H_2(j = 0)$, at $T = 10$, 30, and 80 K. The coupled channels (CC) results are from the present study, the infinite-order-sudden (IOS) values are from Hily-Blant et al. (2013).

	10 K		30 K		80 K	
$N, j, F_1, F \rightarrow N', j', F_1', F'$	CC	IOS	CC	IOS	CC	IOS
$1,\frac{1}{2},1,0 \rightarrow 0,\frac{1}{2},0,1$	4.89(−12)	1.54(−12)	4.27(−12)	1.46(−12)	3.28(−12)	1.07(−12)
$1,\frac{1}{2},1,2 \rightarrow 0,\frac{1}{2},1,2$	2.45(−12)	2.31(−12)	2.13(−12)	2.19(−12)	1.64(−12)	1.61(−12)
$1,\frac{3}{2},1,1 \rightarrow 1,\frac{1}{2},1,2$	1.10(−11)	1.16(−11)	1.48(−11)	1.44(−11)	2.29(−11)	2.00(−11)
$2,\frac{3}{2},2,2 \rightarrow 0,\frac{1}{2},0,1$	4.71(−12)	4.64(−12)	6.86(−12)	7.00(−12)	1.12(−11)	1.12(−11)
$2,\frac{3}{2},2,2 \rightarrow 1,\frac{3}{2},2,2$	1.42(−12)	1.25(−12)	1.13(−12)	1.06(−12)	6.65(−13)	6.30(−13)
$2,\frac{5}{2},2,1 \rightarrow 1,\frac{3}{2},2,3$	1.51(−13)	9.98(−13)	9.92(−14)	9.30(−13)	5.00(−14)	5.29(−13)
$4,\frac{9}{2},5,6 \rightarrow 2,\frac{5}{2},3,4$	3.51(−11)	3.58(−11)	4.25(−11)	3.98(−11)	5.31(−11)	5.35(−11)
$4,\frac{9}{2},5,6 \rightarrow 3,\frac{7}{2},4,5$	5.57(−12)	3.51(−12)	5.02(−12)	4.43(−12)	4.05(−12)	3.75(−12)
$4,\frac{9}{2},5,6 \rightarrow 4,\frac{9}{2},4,5$	2.83(−12)	8.83(−13)	4.87(−12)	1.30(−12)	5.11(−12)	2.10(−12)

Table A2. Illustrative comparisons of rate coefficients ($cm^3\ mol^{-1}\ s^{-1}$) for hyperfine transitions in $C^{15}N$, induced by para-$H_2(j = 0)$, at $T = 10$, 30, and 80 K. The coupled channels (CC) results are from the present study, the infinite–order–sudden (IOS) values are from Hily-Blant et al. (2013).

	10 K		30 K		80 K	
$N, j, F \rightarrow N', j', F'$	CC	IOS	CC	IOS	CC	IOS
$1,\frac{1}{2},1 \rightarrow 0,\frac{1}{2},0$	4.99(−14)	1.54(−12)	3.90(−14)	1.46(−12)	1.92(−14)	1.07(−12)
$1,\frac{3}{2},2 \rightarrow 0,\frac{1}{2},1$	4.82(−12)	4.59(−12)	4.80(−12)	4.35(−12)	3.79(−12)	3.20(−12)
$1,\frac{3}{2},2 \rightarrow 1,\frac{3}{2},1$	5.89(−12)	3.48(−12)	6.36(−12)	5.28(−12)	8.21(−12)	8.40(−12)
$2,\frac{5}{2},2 \rightarrow 0,\frac{1}{2},0$	6.46(−12)	6.96(−12)	1.02(−11)	1.06(−11)	1.67(−11)	1.68(−11)
$2,\frac{5}{2},2 \rightarrow 1,\frac{3}{2},1$	8.89(−12)	8.66(−12)	9.43(−12)	8.21(−12)	5.90(−12)	4.90(−12)
$2,\frac{5}{2},2 \rightarrow 2,\frac{3}{2},1$	4.66(−12)	4.93(−12)	4.87(−12)	4.71(−12)	5.80(−12)	5.38(−12)
$4,\frac{9}{2},5 \rightarrow 2,\frac{5}{2},3$	3.60(−11)	3.63(−11)	4.27(−11)	4.31(−11)	5.38(−11)	5.41(−11)
$4,\frac{9}{2},5 \rightarrow 3,\frac{7}{2},4$	3.42(−12)	3.56(−12)	5.48(−12)	4.49(−12)	4.92(−12)	3.78(−12)
$4,\frac{9}{2},5 \rightarrow 4,\frac{9}{2},4$	1.31(−12)	1.02(−12)	2.02(−12)	1.48(−12)	2.48(−12)	2.41(−12)

This paper has been typeset from a TEX/LATEX file prepared by the author.